



Thermal decomposition and thermal kinetic simulation of ammonium 3,3'-dinitrimino-5,5'-bis(1H-1,2,4-triazole)

Fang Bao¹ · Shaohua Jin¹ · Yi Li¹ · Shusen Chen¹ · Kun Chen¹

Received: 28 December 2019 / Accepted: 3 July 2020 / Published online: 21 July 2020
© Akadémiai Kiadó, Budapest, Hungary 2020

Abstract

Ammonium 3,3'-dinitrimino-5,5'-bis(1H-1,2,4-triazole) (ADNABT) was synthesized and characterized by IR spectroscopy, ¹H/¹³C NMR and single-crystal X-ray diffraction. The thermal decomposition of ADNABT was investigated by thermogravimetry–differential thermal analysis (TG–DTA) and accelerating rate calorimeter (ARC). The kinetic parameters (activation energy, pre-exponential factor, mechanism functions) by DTA and ARC tests were simulated by Thermal Safety Software (TSS). The simulated results revealed that the exothermic decomposition of ADNABT under non-isothermal and adiabatic conditions all followed a full autocatalysis model. In order to ensure the safety of production, transportation and storage, several thermal hazard indicators such as time to maximum rate (TMR), reaction temperature at which TMR is 24 h (T_{D24}), time to conversion limit and self-accelerating decomposition temperature (SADT) were also simulated by TSS on the kinetic model. The T_{D24} and $SADT_{50\text{ kg}}$ were calculated as 183.37 and 167.00 °C, respectively.

Keywords ADNABT · Kinetic simulation · TSS · Thermal hazards · TG–DTA · ARC

Introduction

Nitrogen-rich energetic compounds based on heterocyclic energetic anions, as a prominent family of novel energetic materials, have attracted considerable attention owing to their excellent detonation properties and good stability [1–5]. Heterocyclic energetic anions possess aromatic ring skeletons and large numbers of C–N and N–N bonds which can possess good stability and release more energy. In general, the introduction of nitrogen-rich cations can increase the nitrogen content and performance.

Ammonium 3,3'-dinitrimino-5,5'-bis(1H-1,2,4-triazole) (ADNABT) has been described in the literature previously [1]. The detonation velocity (9407 m s⁻¹) and pressure (34.9 GPa) of ADNABT were similar to that of RDX and HMX and deemed as a promising energetic material. However, the structural characterization by IR spectroscopy, ¹H/¹³C NMR and single-crystal X-ray diffraction was not

mentioned, and its thermal safety properties have not been evaluated.

The purpose of this study was to determine the thermal decomposition and kinetic parameters of ADNABT and provide some thermal hazard indicators for production, transportation and storage. First, the thermal decomposition processes of ADNABT was investigated by thermogravimetry–differential thermal analysis (TG–DTA). Next, the heat capacities (C_p) of ADNABT were measured by difference scanning calorimeter (DSC). The non-isothermal decomposition was measured by DTA at different heating rates. The adiabatic decomposition was measured by accelerating rate calorimeter (ARC) in heat-wait-search mode. Then, the kinetic parameters by DTA and ARC tests were simulated by Thermal Safety Software (TSS) [6–12]. Finally, several thermal hazard indicators such as time to maximum rate (TMR), reaction temperature at which TMR is 24 h (T_{D24}) and time to conversion limit (TCL) and self-accelerating decomposition temperature (SADT) were simulated by TSS on kinetic models [6–12].

✉ Shaohua Jin
jinshaohua@bit.edu.cn

✉ Kun Chen
kchen@bit.edu.cn

¹ School of Materials Science and Engineering, Beijing Institute of Technology, Beijing, China

Experimental

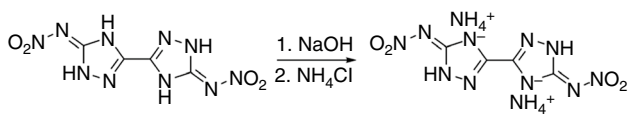
Materials

3,3'-dinitrimino-5,5'-bis(1H-1,2,4-triazole) (DNABT) was homemade and purified according to the literature [1, 13]. Sodium hydroxide (0.60 g, 15 mmol) was added to a suspension of DNABT (1.92 g, 7.5 mmol) in water (50 mL) at room temperature. The reaction mixture was heated at reflux for 1 h. Then, a solution of ammonia chloride (0.80 g, 15 mmol) in water (5 mL) was added to the reaction mixture and heated at reflux for 1 h. The resulting precipitate was collected by filtration, washed with ethanol and dried at 50 °C to give ADNABT (0.86 g, 39%) (Scheme 1). ADNABT: IR (KBr pellet cm^{-1}) 3342, 3205, 3036, 1628, 1525, 1445, 1439, 1396, 1351, 1281, 1253, 1119, 1087, 1011, 977, 863, 804, 766, 738; ^1H NMR (400 MHz d_6 -DMSO ppm) 9.55, 7.00; ^{13}C NMR (100 MHz d_6 -DMSO ppm) 158.08, 153.39.

Suitable crystals of ADNABT for single-crystal X-ray diffraction were obtained by slow evaporation a solution of ADNABT in dimethyl sulfoxide (DMSO). The crystallographic data and crystal structure are shown in Table 1 and Fig. 1, respectively. The results revealed that one molecule of ADNABT was connected to two molecules of DMSO.

Instruments

A Netzsch difference scanning calorimeter device (DSC200 F3) was used to measure C_p of ADNABT. The sample was heated from 30 to 110 °C with a heating rate of 10 °C min^{-1} under a nitrogen flow of 50 mL min^{-1} . A Shimadzu DTG-60H simultaneous thermal analyzer was used to record the non-isothermal decomposition of ADNABT. All samples



Scheme 1 The synthesis route of ADNABT

Table 1 Crystallographic data of ADNABT

Parameters	Values	Parameters	Values	Parameters	Values
Formula	$\text{C}_8\text{H}_{22}\text{N}_{12}\text{O}_6\text{S}_2$	$a/\text{Å}$	6.276	h, k, l_{max}	7, 10, 11
Formula mass/ g mol^{-1}	446.50	$b/\text{Å}$	8.214	R_1, wR_2	0.0507, 0.1178
Crystal system	Anorthic	$c/\text{Å}$	9.705	S	1.278
Space group	P-1	α°	93.49	Z	1
$\lambda_{\text{Mo-K}\alpha}/\text{Å}$	0.71073	β°	97.91	Reflections	1835
T/K	193	γ°	105.35	No. parameters	149
Calculated density/ g cm^{-3}	1.559	Volume/ Å^3	475.46	Device type	Oxford Xcalibur3 CCD

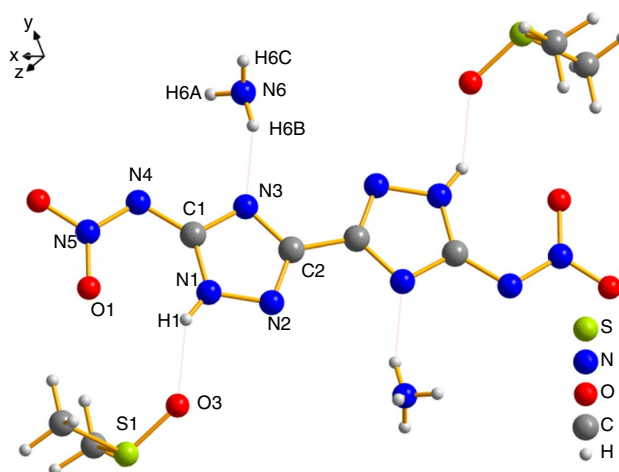


Fig. 1 Crystal structure of ADNABT. Thermal ellipsoids are set to 50% probability. Selected bond lengths/ Å : C1–N1 1.345(34), C1–N3 1.343(39), C2–N2 1.314(39), C2–N3 1.358(31), N3–H6B 1.983(347), N1–H1 0.816(387), H1...O3 2.010(360). Selected bond angles/ $^\circ$: N1–C1–N3 107.39(230), N1–C1–N4 133.77(239), N2–C2–N3 113.90(225), C1–N4–N5 116.50(240). Selected torsion angles/ $^\circ$: C2–N3–C1–N4 178.89(250), N3–C1–N4–N5 179.56(240), N2–N1–H1...O3 4.90(7647), N2–C2–N3...H6B 172.61(1782)

were 1.5 mg and were heated from 50 to 400 °C at different heating rates of 2, 4, 6, 8 °C min^{-1} , respectively. A THT accelerating rate calorimeter (ARC) [14–17] was used to record the adiabatic test of ADNABT. The sample was 100.3 mg and was heated from 80 to 350 °C in heat-wait-search mode. The heat steps and wait times were 15 °C and 15 min, respectively.

Results and discussion

Thermal decomposition processes by TG–DTA test

TG–DTA curve of ADNABT under a heating rate of 8 °C min^{-1} is shown in Fig. 2. Obviously, there were two significant peaks, among which, the first endothermic peak ranges from 122.53 to 168.35 °C with a mass loss of 36.0%, and the second exothermic peak ranges from 216.40 to 278.05 °C with a mass loss of 32.2%. The theoretically

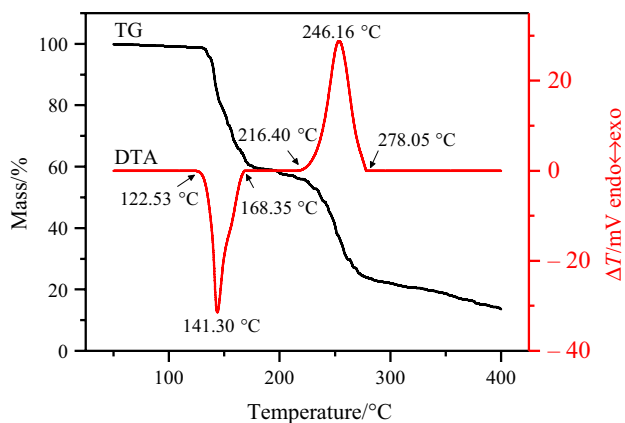


Fig. 2 TG–DTA curve of ADNABT at a heating rate of 8 °C min⁻¹

calculated mass loss of DMSO was 35.0%, and that was similar to the mass loss of first endothermic peak. Hence, the first endothermic peak was a process of lost DMSO.

Heat capacity by DSC test

The relationship between C_p and T of ADNABT was established by four steps. First, get the values of C_p by DSC. Next, open the ARKS-CK of TSS, and input the needed parameters, such as formula, density, temperature and C_p . Then, press calculator button, the relationship between C_p and T was simulated on the default model ($C_p = a_0 + a_1T + a_2T^2$). Finally, get the calculated results of a_0 , a_1 and a_2 . Thus, we got the relationship between C_p and T , and the simulated C_p is shown in Fig. 3. The C_p of ADNABT at 298.15 K is calculated as 1.277 J g⁻¹ K⁻¹. The relationships between C_p and T were described as follows:

$$C_p = 1.540 \times 10^{-1} - 4.119 \times 10^{-3} \times T + 1.070 \times 10^{-6} \times T^2 \tag{1}$$

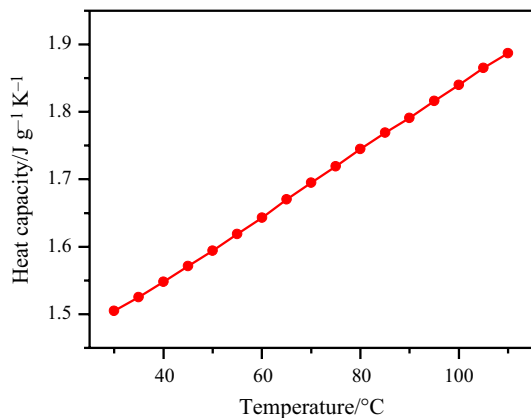


Fig. 3 Simulated heat capacity of ADNABT by DSC test

Kinetic simulation by DTA test

DTA curves of ADNABT under different heating rates (β) of 2, 4, 6 and 8 °C min⁻¹ are shown in Fig. 4. The experimental parameters, such as onset temperature (T_o), peak temperature (T_p), endset temperature (T_e) and heat production (Q), are listed in Table 2. The DTA results revealed that the heights and areas of first endothermic and second exothermic peaks were increased when the heating rates were raised.

Most simulation of kinetic models involves complex multi-stage reactions, which consist of several of independent, parallel and consecutive stages. The simple, n th-order and autocatalytic kinetic models for a single-stage reaction ($A \rightarrow B$) were presented in Eqs. (2)–(4), respectively [8, 18–21].

$$\frac{d\alpha}{dt} = k_0 \exp\left(-\frac{E}{RT}\right) f(\alpha) \tag{2}$$

$$\frac{d\alpha}{dt} = k_0 \exp\left(-\frac{E}{RT}\right) (1 - \alpha)^n \tag{3}$$

$$\frac{d\alpha}{dt} = k_0 \exp\left(-\frac{E}{RT}\right) (1 - \alpha)^{n_1} (\alpha^{n_2} + z) \tag{4}$$

where α is the degree of conversion; t is the time; k_0 is the pre-exponential factor; E is the activation energy; R is ideal gas constant; T is the temperature; n_1 , n_2 and n are the reaction orders of a specific stage; z is autocatalytic constant.

The kinetic models that include two consecutive stages ($A \rightarrow B \rightarrow C$) were described as follows [8, 18–21]:

$$\frac{d\alpha}{dt} = k_1 \exp\left(-\frac{E_1}{RT}\right) (1 - \alpha)^{n_1} \tag{5}$$

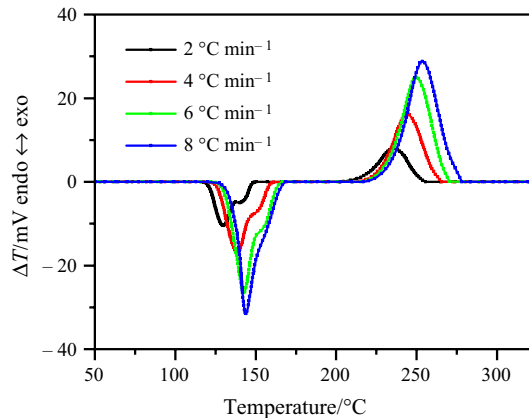


Fig. 4 Thermal decomposition curves of ADNABT by DTA test

$$\frac{d\gamma}{dt} = k_2 \exp\left(-\frac{E_2}{RT}\right)(\alpha - \gamma)^{n_2} \quad (6)$$

where α and γ are the degree of conversion of stage one and two, respectively; k_1 and k_2 are the pre-exponential factors of stage one and two, respectively; E_1 and E_2 are the activation energies of stage one and two, respectively; n_1 and n_2 are the reaction orders of stage one and two, respectively.

The kinetic models for two parallel reactions ($A \rightarrow B$; $A + B \rightarrow 2B$) were described as follows [8, 18–21]:

$$\begin{aligned} \frac{d\alpha}{dt} = r_1(\alpha) + r_2(\alpha) = & k_{01} \exp\left(-\frac{E_1}{RT}\right)(1 - \alpha)^{n_{11}} \\ & + k_{02} \exp\left(-\frac{E_2}{RT}\right)\alpha^{n_{21}}(1 - \alpha)^{n_{22}} \end{aligned} \quad (7)$$

where r_1 and r_2 are the rates of stage one and two, respectively.

Assuming that $n_{11} = n_{22} = n_1$ and $n_{21} = n_2$, then the kinetic model of full autocatalysis can be described as follows [20, 21]:

$$\frac{d\alpha}{dt} = k_0 \exp\left(-\frac{E}{RT}\right)(1 - \alpha)^{n_1} \left[z_0 \exp\left(-\frac{E_z}{RT}\right) + \alpha^{n_2} \right] \quad (8)$$

where z_0 is the ratio of pre-exponential factor k_{01}/k_{02} ; E_z is the difference E_1 and E_2 .

The kinetic parameters of ADNABT by DTA tests were simulated by TSS, and the results are listed in Table 3. The simulated and experimental values of heat production rate and heat production are shown in Fig. 5. The simulated values of heat production rate and heat production were similar to the experimental values. Hence, It could be concluded that the exothermic decomposition of ADNABT under non-isothermal conditions followed a full autocatalysis model.

Kinetic simulation by ARC test

The exothermic decomposition of ADNABT by ARC is shown in Fig. 6. The experimental parameters such as onset temperature, final temperature, adiabatic temperature rise, max self-heating rate, max pressure and so on are listed in Table 4. The endothermic decomposition of loss DMSO

Table 2 Experimental parameters of ADNABT by DTA tests

$\beta/^\circ\text{C min}^{-1}$	$T_{o1}/^\circ\text{C}$	$T_{p1}/^\circ\text{C}$	$T_{e1}/^\circ\text{C}$	$Q_1/\text{J g}^{-1}$	$T_{o2}/^\circ\text{C}$	$T_{p2}/^\circ\text{C}$	$T_{e2}/^\circ\text{C}$	$Q_2/\text{J g}^{-1}$
2	115.54	124.47	150.18	-4742	201.03	230.26	255.98	3442
4	118.82	131.86	161.67	-4431	206.69	236.45	265.63	3503
6	120.88	140.03	166.43	-2869	214.19	242.60	270.44	3666
8	122.53	141.30	168.53	-2309	216.40	246.16	278.05	3324

Table 3 The simulated kinetic parameters of ADNABT by DTA tests

Compound	$\ln k_0/\ln\text{s}^{-1}$	$E/\text{kJ mol}^{-1}$	n_1	n_2	$\ln z_0$	$E_z/\text{kJ mol}^{-1}$	$Q/\text{J g}^{-1}$
ADNABT	39.56	189.39	1.33	0.47	-3.91	9.16	3470

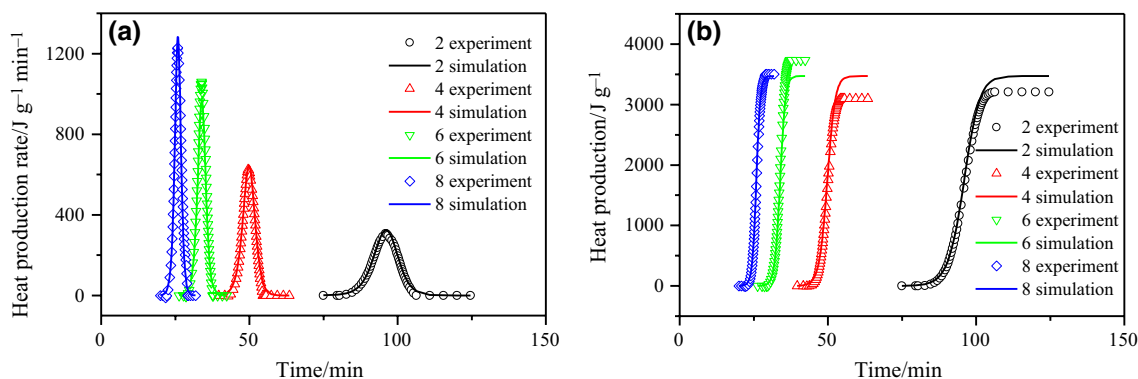


Fig. 5 Simulated and experimental heat product rate and heat production of ADNABT by DTA tests. **a** Heat production rate versus time, **b** heat production versus time

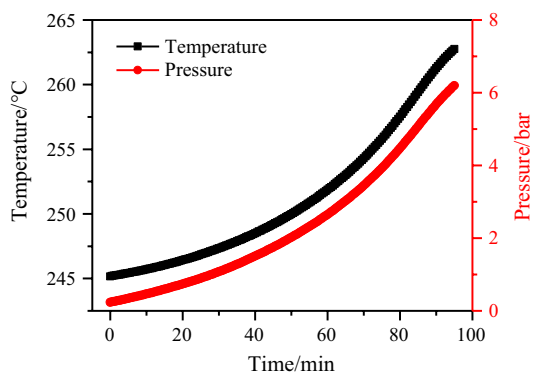


Fig. 6 The exothermic decomposition curve of ADNABT by ARC test

was between 148.25 and 156.08 °C, and the pressure was increased by 8.64 bar. The exothermic decomposition of ADNABT started at 245.17 °C and ended at 264.28 °C, and the pressure was increased by 6.48 bar.

The kinetic parameters of ADNABT were evaluated by AC and FK of TSS. The kinetic model of ADNABT by ARC test was described as Eq. (8). The simulated results such as E , $\ln k_0$, n , Q are listed in Table 5. The simulated and experimental values of heat production rate, heat production, gas production rate and gas production of ADNABT by ARC test are shown in Fig. 7. The simulated values of heat production rate, heat production, gas production rate and gas production were similar to the experimental values which revealed that the simulated results were credible. From the simulated results by using TSS, It could be concluded that the exothermic decomposition of ADNABT by ARC test also followed a full autocatalysis model.

TMR is the time instant when reaction reaches its maximal rate under adiabatic conditions which was proposed by Townsend and Tou [22], and their method was only suitable for simple single-stage n -order reactions. In the case of more complex reactions (including autocatalytic reactions), TMR can be properly determined merely by applying a kinetic-based simulation [6, 23–27]. T_{D24} is the reaction temperature at which TMR is 24 h [6]. The kinetic parameters of ADNABT were got from Table 5. The TMR was estimated by applying a kinetic-based simulation, and the simulated TMR is shown in Fig. 8. The TMR at 150 °C was calculated as 109.38 days, and the T_{D24} was calculated as 183.37 °C.

Assessment of thermal stability of a substance (stability analysis) lies in evaluating the dependency of time instant (time to conversion limit, TCL) when conversion of a reaction reaches some predefined value-conversion limit, at constant set temperature [6, 23–27]. Thermal stability is essentially characterized by the time of TCL necessary to reach a certain level of conversion at a specific constant temperature. Therefore, for long-term storage, it can be selected as the maximum permissible time during which the conversion of the product does not have any prominent impact on the product quality. The TCL (10% conversion limit) was estimated by applying a kinetic-based simulation, and the simulated TCL is shown in Fig. 8. The TCL (10% conversion limit) at 150 °C was calculated as 25.68 days.

SADT is defined as the lowest ambient air temperature at which self-accelerating decomposition may occur within a substance in the packaging as used in transport and storage. Assuming 50 kg ADNABT was loaded in a steel barrel with heat 40 cm and radius 15 cm. SADT was evaluated by ThermEx of TSS. The $SADT_{50\text{ kg}}$ was calculated as 167.00 °C.

Table 4 Experimental parameters of ADNABT by ARC test

Parameters	ADNABT	Parameters	ADNABT
Onset temperature/°C	245.17	Max pressure/bar	6.48
Onset temperature rate/°C min ⁻¹	0.06	Max pressure rise rate/bar min ⁻¹	0.10
Temperature at max rate/°C	257.49	Thermal inertia factor	31.26
Max self-heating rate/°C min ⁻¹	0.30	Total gas production/mol kg ⁻¹	11.91
Final temperature/°C	264.28	Decomposition enthalpy/J g ⁻¹	832.19
Adiabatic temperature rise/°C	19.11		

Table 5 The kinetic parameters of ADNABT by ARC test

Compound	$\ln k_0/\ln s^{-1}$	$E/\text{kJ mol}^{-1}$	n_1	n_2	$\ln z_0$	$E_z/\text{kJ mol}^{-1}$	$Q/\text{J g}^{-1}$	$G/\text{mol kg}^{-1}$
ADNABT	29.15	157.87	1.09	1.33	-0.13	9.49	950	12.59

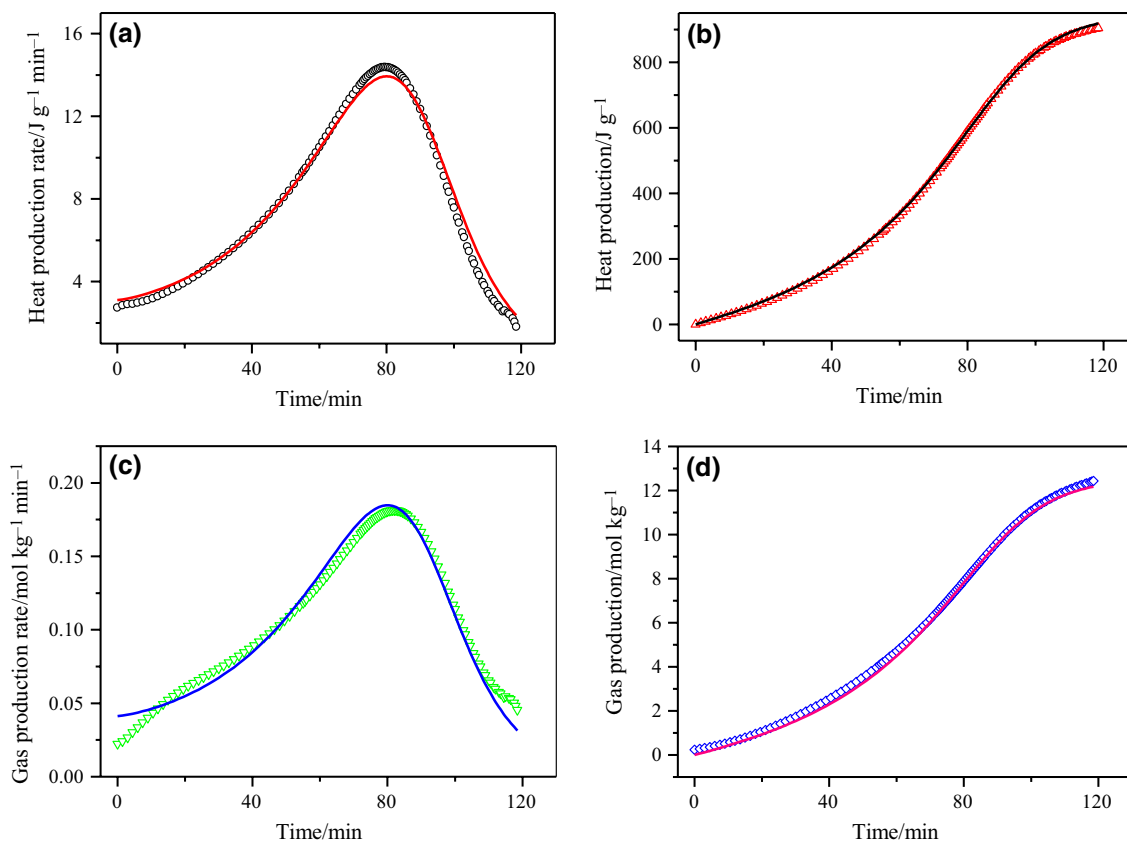


Fig. 7 Simulated and experimental heat production rate, heat production, gas production rate and gas production of ADNABT by ARC test. **a** Heat production rate versus time, **b** heat production versus time, **c** gas production rate versus time, **d** gas production versus time

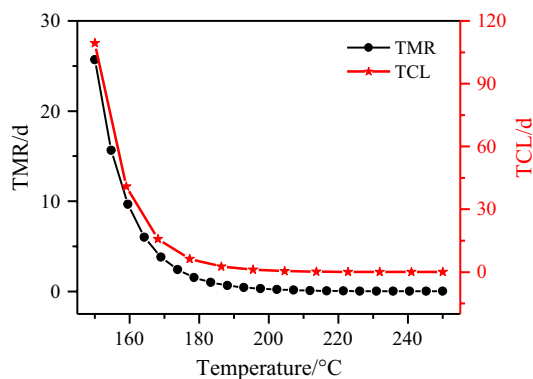


Fig. 8 Simulated TMR and TCL of ADNABT by ARC test

Conclusions

In conclusion, the thermal decomposition of ADNABT was performed by TG–DTA and ARC, and these tests data were simulated by TSS. The results were reported in detail.

1. The TG–DTA measurement showed that ADNABT has two decomposition processes, and the first process is an endothermic decomposition of loss DMSO, and the second process is an exothermic decomposition. The kinetic parameters of exothermic decomposition such as E , k_0 and $f(\alpha)$ were evaluated by TSS. The exothermic decomposition of ADNABT under non-isothermal conditions followed a full autocatalysis model.
2. The ARC measurement also showed that ADNABT has an endothermic and an exothermic decomposition. The kinetic parameters of exothermic decomposition such as E , k_0 and $f(\alpha)$ were also simulated by TSS, and the results indicated that the exothermic decomposition of ADNABT under adiabatic condition also followed a full autocatalysis model. The several thermal hazard indicators such as TMR, T_{D24} , TCL and SADT were also simulated by TSS on kinetic model. The TMR and TCL (10% conversion limit) at 150 °C were calculated as 109.38 and 25.68 days, respectively. The T_{D24} and $SADT_{50\text{ kg}}$ were calculated as 183.37 and 167.00 °C, respectively.

References

1. Wang RH, Xu HY, Guo Y, Sa RJ, Shreeve JM. Bis[3-(5-nitroimino-1,2,4-triazolate)]-based energetic salts: synthesis and promising properties of a new family of high-density insensitive materials. *J Am Chem Soc.* 2010;132:11904–5.
2. Fischer N, Izsák D, Klapötke TM, Rappenglück S, Stierstorfer J. Nitrogen-rich 5,5'-bistetrazolates and their potential use in propellant systems: a comprehensive study. *Chem Eur J.* 2012;18:4051–62.
3. Dippold AA, Klapötke TM, Winter N. Insensitive nitrogen-rich energetic compounds based on the 5,5'-dinitro-3,3'-bi-1,2,4-triazole-2-ide anion. *Eur J Inorg Chem.* 2012;21:3474–84.
4. Dippold AA, Klapötke TM. A study of dinitro-bis-1,2,4-triazole-1,1'-diol and derivatives: design of high-performance insensitive energetic materials by the introduction of N-oxides. *J Am Chem Soc.* 2013;135:9931–8.
5. Dippold AA, Klapötke TM, Oswald M. Asymmetrically substituted 5,5'-bistriazoles-nitrogen-rich materials with various energetic functionalities. *Dalton Trans.* 2013;42:11136–45.
6. Rao GN, Feng W, Zhang J, Wang SY, Chen LP, Guo ZC, Chen WH. Simulation approach to decomposition kinetics and thermal hazards of hexamethylenetetramine. *J Therm Anal Calorim.* 2019;135:2447–56.
7. Mi WZ, Wei RC, Zhou TN, He JJ, Wang J. Experimental study on the thermal decomposition of two nitrocellulose mixtures in different forms. *Mater Sci Medzg.* 2019;25:60–5.
8. Wei RC, Huang SS, Wang Z, He Y, Yuen R, Wang J. Estimation on the safe storage temperature of nitrocellulose with different humectants. *Propellants, Explos, Pyrotech.* 2018;43:1122–8.
9. Gan XY, Yang S, Wang SY, Guo XY, Chen LP, Chen WH. Thermal behavior of benzoyl peroxide mixed with NaOH solution. *Thermochim Acta.* 2018;670:13–7.
10. Shen SJ, Wu SH, Chi JH, Lin CC, Horng JJ, Shu CM. Simulation of solid thermal explosion and liquid thermal explosion of dicumyl peroxide using calorimetric technique. *Simul Model Pract Theory.* 2011;19:1251–7.
11. Shen SJ, Wu SH, Chi JH, Wang YW, Shu CM. Thermal explosion simulation and incompatible reaction of dicumyl peroxide by calorimetric technique. *J Therm Anal Calorim.* 2010;102:569–77.
12. You ML, Liu MY, Wu SH, Chi JH, Shu CM. Thermal explosion and runaway reaction simulation of lauroyl peroxide by DSC tests. *J Therm Anal Calorim.* 2009;96:777–82.
13. Dippold AA, Klapötke TM. Nitrogen-rich bis-1,2,4-triazoles-a comparative study of structural and energetic properties. *Chem Eur J.* 2012;18:16742–53.
14. Zhang CY, Jin SH, Chen SS, Li LJ, Zhou C, Zhang Y, Shu QH. Thermal behavior and thermo-kinetic studies of 5,5'-bistetrazole-1,1'-diolate (1,1-BTO). *J Therm Anal Calorim.* 2017;129:1265–70.
15. Bao F, Zhang GZ, Jin SH. Thermal decomposition behavior and thermal stability of DABT-2DMSO. *J Therm Anal Calorim.* 2018;131:3185–91.
16. Bao F, Zhang GZ, Jin SH, Zhang CY, Niu H. Thermal decomposition and safety assessment of 3,3'-dinitrimino-5,5'-bis(1H-1,2,4-triazole) by DTA and ARC. *J Therm Anal Calorim.* 2018;132:805–11.
17. Vyazovkin S, Burnham AK, Criado JM, Pérez MLA, Popescu C, Sbirrazzuoli N. ICTAC kinetics committee recommendations for performing kinetic computations on thermal analysis data. *Thermochim Acta.* 2011;520:1–19.
18. Lin HY, Tsai SY, Tseng YL, Lin CP. Gamma irradiation for improving functional ingredients and determining the heat treatment conditions of *Cordyceps militaris* mycelia. *J Therm Anal Calorim.* 2015;120:439–48.
19. Tseng JM, Lin CP. Prediction of incompatible reaction of dibenzoyl peroxide by isothermal calorimetry analysis and green thermal analysis technology. *J Therm Anal Calorim.* 2012;107:927–33.
20. Kossoy AA, Belokhvostov VM, Koludarova EY. Thermal decomposition of AIBN: part D: verification of simulation method for SADT determination based on AIBN benchmark. *Thermochim Acta.* 2015;621:36–43.
21. Cao CR, Liu SH, Das M, Shu CM. Evaluation for the thermokinetics of the autocatalytic reaction of cumene hydroperoxide mixed with phenol through isothermal approaches and simulations. *Process Saf Environ.* 2018;117:426–38.
22. Townsend DI, Tou JC. Thermal hazard evaluation by an accelerating rate calorimeter. *Thermochim Acta.* 1980;37:1–30.
23. Kossoy A, Sheinman I. Effect of temperature gradient in sample cells of adiabatic calorimeters on data interpretation. *Thermochim Acta.* 2010;500:93–9.
24. Kossoy AA, Singh J, Koludarova EY. Mathematical methods for application of experimental adiabatic data—an update and extension. *J Loss Prevent Proc.* 2015;33:88–100.
25. Hsueh KH, Chen WT, Chu YC, Tsai LC, Shu CM. Thermal reactive hazards of 1,1-bis(tert-butylperoxy) cyclohexane with nitric acid contaminants by DSC. *J Therm Anal Calorim.* 2012;109:1253–60.
26. Tsai SY, Lin HY, Hong WP, Lin CP. Evaluation of preliminary causes for vitamin D series degradation via DSC and HPLC analyses. *J Therm Anal Calorim.* 2017;130:1357–69.
27. Cheng YF, Liu SH, Shu CM, Zhang B, Li YF. Energy estimation and modeling solid thermal explosion containment on reactor for three organic peroxides by calorimetric technique. *J Therm Anal Calorim.* 2017;130:1201–11.

Publisher's Note Springer Nature remains neutral with regard to jurisdictional claims in published maps and institutional affiliations.